Journal of Orthopaedics 13 (2016) 404–408

Contents lists available at ScienceDirect

Journal of Orthopaedics

journal homepage: www.elsevier.com/locate/jor

Original Article

Bone formation of human mesenchymal stem cells harvested from reaming debris is stimulated by low-dose bone morphogenetic protein-7 application *in vivo*

Fabian Westhauser *, Melanie Höllig, Bruno Reible, Kai Xiao, Gerhard Schmidmaier, Arash Moghaddam

HTRG – Heidelberg Trauma Research Group, Trauma and Reconstructive Surgery, Center of Orthopedics, Traumatology, and Spinal Cord Injury, Heidelberg University Hospital, Schlierbacher Landstraße 200a, D-69118 Heidelberg, Germany

ARTICLE INFO

Article history:
Received 1 August 2016
Accepted 15 August 2016
Available online 29 August 2016

Keywords:
Tissue engineering
Human mesenchymal stem cells (MSC)
Bone morphogenetic protein-7 (BMP-7)
Micro-computed tomography (mCT)
Reaming material

ABSTRACT

Stimulation of mesenchymal stem cells (MSC) by bone morphogenetic protein-7 (BMP-7) leads to superior bone formation *in vitro*. In this *in vivo*-study we evaluated the use of BMP-7 in combination with MSC isolated from reaming debris (RIA-MSC) and iliac crest bone marrow (BMSC) with micro-computed tomography (mCT)-analysis.

β-Tricalciumphosphate scaffolds coated with BMSC and RIA-MSC were stimulated with three different BMP-7-concentrations and implanted ectopically in severe combined immunodeficiency (SCID) mice.

Our results demonstrate that RIA-MSC show a higher osteogenic potential *in vivo* compared to BMSC. Ossification increased in direct correlation with the BMP-7-dose applied, however low-dose-stimulation by BMP-7 was more effective for RIA-MSC.

1. Introduction

Bone healing disorders and the treatment of bone defects are still amongst the most challenging and common disorders in orthopedic surgery.[1,2] Tissue engineering protocols for the treatment of bone defects include the use of autologous cell populations in combination with differentiation factors such as bone-morphogenetic-protein 7 (BMP-7) to promote local bone healing processes.[3]

The gold standard for harvesting mesenchymal stem cells (MSC) is iliac crest bone grafting.[4] However, extensive donor site morbidity and limited extraction quantity diminish use of the iliac crest as a possible source of harvesting MSC.[5] Reaming material (RIA) from the femur proved to be an effective alternative source for harvesting MSC (RIA-MSC).[1] In experimental settings, RIA-MSC showed a significantly better osteogenic differentiation potential *in vivo* compared to MSC harvested from iliac crest bone marrow aspirate (BMSC).[4]

The combination of reaming material and BMP-7 application showed good results clinically.[1] However, there is no evidence concerning the interaction of BMP-7 with human RIA-MSC (hRIA-MSC) nor with human BMSC (hBMSC) using a standardized *in vivo* model. Although there is some evidence that BMP-7 stimulates bone formation of hBMSC *in vitro*, the dose dependent BMP-7 stimulation of hBMSC and hRIA-MSC *in vivo* is even more interesting and less investigated.[6] Furthermore, the treatment of bone defects is still in need of improvement; a balanced combination of MSC and differentiation factors has not yet been found.[7]

In summary, this study focused on evaluating bone formation with hBMSC and hRIA-MSC-coated β-tricalciumphosphate (β-TCP) scaffolds, stimulated with different concentrations of BMP-7 and implanted ectopically in severe combined immunodeficiency (SCID) mice. Bone formation was analyzed using quantitative micro-computed tomography (mCT) analysis as stated in the literature.[7] By using human MSC in an *in vivo* model, results can be transferred more directly to clinical settings.

* Corresponding author.
E-mail address: Fabian.Westhauser@med.uni-heidelberg.de (F. Westhauser).

http://dx.doi.org/10.1016/j.jor.2016.08.002

2. Materials and methods

2.1. Study ethics and patient demography

hBMSC from iliac crest bone marrow aspirate and hRIA-MSC from reaming debris were isolated from nine donors (four males and five females) undergoing bone defect treatment at Heidelberg University Hospital. Both materials were isolated from each donor. The mean age was 50.2 years (range: 20–79 years). Reaming material was harvested using the Reamer-Irrigator-Aspirator (RIA) System (Synthes GmbH, Umkirch, Germany).[1] Informed consent was obtained according to the declaration of Helsinki in its present form.[8] We did not match the donor collective to factors that could influence MSC quality in order to improve transferability to clinical routine.[9] This study was approved by the ethics committee of the Ruprecht-Karls-University of Heidelberg (S-355/2010).

2.2. hMSC characteristics, isolation and cultivation

Bone marrow aspirate was harvested from the anterior iliac crest of the patient, and RIA from the patient's femur. Isolation, cultivation, and expansion of hBMSC and hRIA-MSC was conducted according to standardized protocols as published previously.[4,7,10] The definition of the cells as MSC was carried out by flow cytometry, plastic adherence, and trilineage differentiation.[10]

2.3. β-TCP scaffold preparation

One million MSC (hBMSC or hRIA-MSC) were seeded dynamically on β-TCP granules as published before.[2,4] 10 mg phase-pure β-TCP was used as scaffold material, with a granule size of 0.5–0.7 μm and a porosity of 60% (RMS Foundation, Bettlach, Switzerland). After seeding, fibrin/thrombin-tissue-glue (Baxter Deutschland GmbH, Unterschleißheim, Germany) was applied to the granules to form a solid construct (Fig. 1a). For each donor, 12 constructs were built in total: six seeded with hBMSC ("BM") and six with hRIA-MSC ("RIA"). Two constructs were built without BMP-7-stimulation ("BM0" and "RIA0", respectively), two with 0.1 μg/ml BMP-7 ("BM0.1" and "RIA0.1", respectively) (Olympus Biotech Europe, Lyon, France) and two with 1.0 μg/ml BMP-7 ("BM1" and "RIA1", respectively). Additionally, we implanted each two constructs without cells under stimulation with three different BMP-7-doses to exclude bone formation induced by the host ("control group").

2.4. Animal model and surgical procedure

SCID-mice (CB17/Icr-Prkdc^{scid}/Crl, Charles River, Wilmington, MA) were used as hosts for scaffolds seeded with human MSC. The SCID-model has been published before.[4,7] The regional Council of Karlsruhe approved the use of animals (35-9185.81/G-251/12) according to the regulations from the European Laboratory Animal Science Guidelines.

In brief, mice were anaesthetized. Four scaffolds were implanted into one mouse on the back, over the anterior and posterior limbs in subcutaneous pouches (Fig. 2d). Mice were sacrificed by cervical dislocation after eight weeks and scaffolds were explanted (Fig. 1b).

2.5. mCT acquisition and evaluation

Prior to implantation (T0) and after explantation (T1) of the constructs, mCT-scans were provided. A SkyScan 1076 Hasitom (Bruker, Billerica, MA) with a tube current of 200 μA, an integration time of 420 ms, and voltage of 50 kVp was used to perform mCT-scans. Pixel size was 17.7 μm. A 0.5 mm aluminum filter was used to absorb the low-energy part of the generated X-ray spectrum. During the scanning-procedure, samples were stored in PBS-filled kryovials (Eppendorf AG, Hamburg, Germany) according to current recommendations.[11] NRecon (Skyscan, Kontich, Belgium) was used for 3D-reconstruction. Beam hardening correction (BHC) = 10 and ring artifacts reduction (RAR) = 6 were applied to the datasets. Misalignment compensation was adapted individually to each construct. For quantitative mCT-analysis, Heidelberg-mCT-Analyzer was used to evaluate the scaffold's properties.[7] Although, Heidelberg-mCT-Analyzer offers a lot of parameters to analyze bone formation, we decided to use a specific set of parameters appropriate to illustrate the changes within the constructs over time. Total volume (TV) represents the whole construct including soft tissue. Scaffold volume (SV) reduces the dataset after segmentation to the scaffold itself, excluding soft tissue. Scaffold surface (SS) represents the construct's surface. Porosity (*P*) describes the ratio of TV to the volume of empty spaces within the construct. The pore number (PN) represents the total amount of pores within the scaffold. The relevant pore number (rPN) is a part of PN and shows the number of pores with a diameter between 100 and 500 μm. According to the literature, this specific subset of pores allows for bone ingrowth.[12] Furthermore, the mCT-slices were analyzed qualitatively by at least two of the authors to confirm radiological correlates of tissue mineralization and bone formation.

2.6. Histomorphometry

Histomorphometric analysis was used to evaluate bone formation after T1 mCT-acquisition by HE stain qualitatively (Carl Roth, Karlsruhe, Germany) according to literature.[2,4]

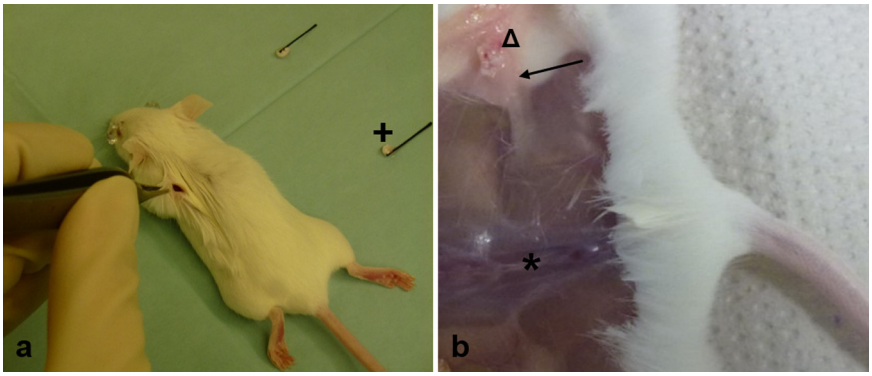

Fig. 1. Implantation (a) and explantation (b) of the constructs. (a) Implantation of the constructs (+) at the back lateral of the spine (*) over the anterior and posterior limbs in subcutaneous pouches. After eight weeks, constructs were explanted (b). The constructs showed excellent integration into the subcutaneous pouch (→) and showed signs of vascularization (Δ).

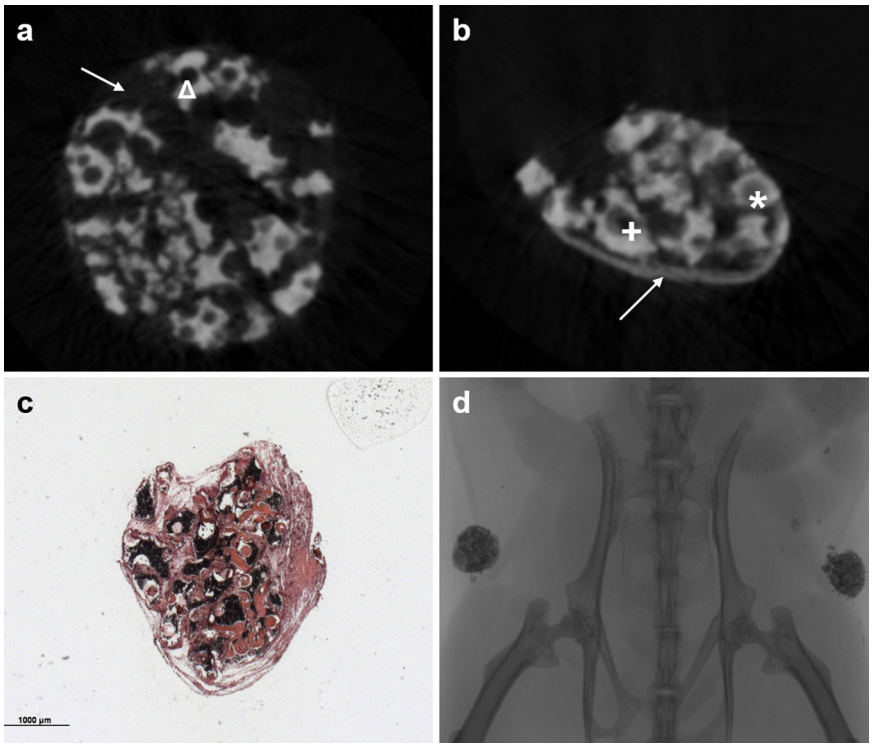

Fig. 2. Ectopic bone formation: (a) One representative construct at T0 is shown: β-TCP-granules (Δ) are clearly seen forming a solid construct. (b) The same construct at time point T1; pores (*) and the spaces between the granules and the periphery of the construct (→) are filled with bone. Even though some "big pores" are not completely filled with bone over time, a smaller pore (+) remains in T1 compared to T0. The construct became compact and dense over time. (c) Histomorphometry shows a dense construct, bone was detectable (*). (d) A mCT-scout scan showing the implants within the animal.

2.7. Statistics

SPSS (IBM Corporation, Armonk, NY) was used for statistical analysis. Results (T0 vs. T1) were analyzed by the *t*-test for paired samples. Results were seen as statistically significant if $p < 0.05$.

3. Results

3.1. Constructs

114 constructs were implanted into 29 SCID-mice (Fig. 1a). Two mice were used for implantation of the constructs of the control-groups.

3.2. In vitro

Both cells isolated from RIA-material and iliac crest aspirate fulfilled the necessary MSC-characteristics: surface antigen expression, plastic adherence and trilineage differentiation.[10]

3.3. Macroscopic findings

Constructs showed excellent integration into the subcutaneous tissue at the time of explantation. Furthermore, vascularization from host to implant could be seen macroscopically (Fig. 1b). The constructs seeded with hMSC became solid, whereas the controls remained as "soft" as they were before implantation.

3.4. Histomorphometry

HE staining revealed new bone within every hBMSC and hRIA-MSC coated construct (Fig. 2c) whereas no bone formation but only fibrous tissue could be found in the control-groups (Fig. 3). Therefore, the changes, described by mCT-analysis could be interpreted as correlates of bone formation.[2]

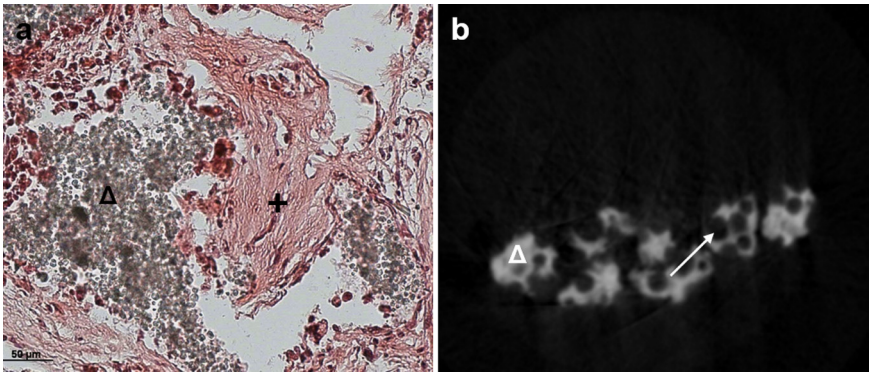

Fig. 3. Control group. (a) In histomorphometry only formation of fibrous tissue (+) around the β-TCP-granules (Δ) was detected. (b) Pores (→) in T1-mCT-analysis were not filled with bone. No bone formation was detected around the β-TCP-granules (Δ).

3.5. Quantitative mCT-analysis

Evaluation of bone formation from T0 to T1 over time was performed by the Heidelberg-mCT-Analyzer.[2] We decided to use an appropriate subset of parameters as described above (Table 1). TV showed significant declines in all groups. SV, representing the scaffold and calcified tissue decreased the most in RIA1 (−16.05%). SV decreased within all groups, but declines were not significant in both BM0 and RIA0. In all groups, SS decreased significantly, whereas the highest decrease was analyzed within RIA1 (−29.41%). P showed only a slight change in RIA1 (−1.06%), and no significant decrease in BM0.1 (−6.67%, $p = 0.087$) and RIA0 (−5.93%, $p = 0.063$). In BM0, BM1, and RIA0.1, decreases for P were significant. P represents the ratio of TV to the volume of empty spaces within the construct ($P = (TV - SV)/TV$). This means it always depends on the properties of TV. PN decreased within all groups, but only the changes in RIA0.1 and RIA1 were significant. The number of pores decreased most in RIA1 (−13.92%). Nearly the same applied for rPN: a non-significant increase was detected in BM0 ($p = 0.705$) and BM0.1 ($p = 0.474$). For BM1 and all the RIA-groups, a significant decrease was observed with a maximum in RIA1 (−18.97%, $p < 0.001$).

For T0, in BM0 76.9% of the total number of pores were part of rPN, in BM0.1 75.5%, in BM1 75.3%, in RIA0 80.3%, in RIA0.1 78.3% and in RIA1 79.1%. For T1, percentage amount of rPN out of PN in BM0 was 78.4%, in BM0.1 78.1%, in BM1 75.8%, in RIA0 75.8%, in RIA0.1 79.4%, and in RIA1 75.7%. That refers to an increase from T0 to T1 in BM0 (1.47%), in BM0.1 (2.57%), in BM1 (0.51%) and in RIA0.1 (1.07%). A decrease was detectable in RIA0 (−4.50%) and RIA1 (−3.36%).

3.6. Qualitative mCT-analysis

All constructs were analyzed qualitatively by two of the authors. Bone formation and calcified tissue was detected within all groups (Fig. 2b). The largest quantity of bone was found in RIA0.1 and RIA1; no calcified tissue was detected within the control groups (Fig. 3b). The RIA-constructs showed a denser and more compact character, compared to the BM-implants. This is also represented by the stronger decline of SS in the RIA-groups, compared to the BM-implants.

4. Discussion

In the presented study, we could show that BMP-7 is able to enhance bone formation of hMSC-coated β-TCP-scaffolds *in vivo*. By analyzing the correlates of bone formation in mCT, hMSC isolated from RIA-material show a slightly higher potential of bone formation compared to hBMSC. This outlines the findings of a previously published study.[4] Furthermore, hRIA-MSC react more sensitively to stimulation by BMP-7, even with low dose-application. Positive aspects of this study include the use of human MSC, and the comparison of hMSC isolated from different tissues. By analyzing bone formation of hMSC *in vivo*, the results of our study are more likely to be transferred into the clinical situation, compared to the use of rodent MSC.[13]

As published before, we were able to show that ectopically implanted hMSC-coated β-TCP-scaffolds allow for bone formation.[4] Within control groups consisting of unseeded scaffolds, no bone formation was detected (Fig. 3). Furthermore, the volume of β-TCP (TV and SV) remained without significant changes over time, thus showed no decline. Therefore, we assume that resorption of β-TCP plays a minor role within our experimental setting compared to the implantation of β-TCP in bone defects as shown before.[14]

By using an established *in vivo* model, we were able to compare the osteogenic potential of hBMSC with that of hRIA-MSC.[2,4] It has been shown in previous studies that ectopically implanted constructs only provide bone formation and do not induce cartilage tissue growth; bone formation within the implants is induced by the implanted human MSC and does not come from the host itself.[15] By comparing RIA0 to BM0, we could detect a significant decrease of rPN in RIA0, but not in BM0. Assuming that the porous character of scaffolds is one of the most important characteristics leading to the promotion of bone ingrowth, changes in rPN are sensitive markers for bone formation. While PN includes pores of all sizes, rPN represents the pores that make bone ingrowth possible. According to literature, a minimal diameter of

Table 1
Quantitative mCT-characteristics of the implants. Table shows mean values. T0 represents the condition at the time of implantation and T1 after explantation. $\Delta\% = 1 - (T0/T1)$ represents the percentage change over time from T0 to T1. p shows the p-values for T0 compared to T1; significant changes are marked (*).

		TV [10^{10} µm^3]	SV [10^{10} µm^3]	SS [10^7 µm^2]	P [1/µm]	PN	rPN
T0	BM0	1.70	5.74	10.11	0.66	937	727
	BM0.1	1.66	5.88	10.11	0.64	955	728
	BM1	1.70	5.75	10.03	0.66	957	725
	RIA0	1.64	5.63	10.05	0.66	935	756
	RIA0.1	1.68	5.72	10.01	0.66	925	725
	RIA1	1.58	5.68	9.97	0.64	931	740
T1	BM0	1.31	5.32	8.55	0.58	911	721
	BM0.1	1.36	5.20	8.63	0.60	909	717
	BM1	1.33	5.53	8.36	0.57	896	685
	RIA0	1.45	5.40	8.37	0.62	898	688
	RIA0.1	1.28	5.15	8.03	0.59	855	679
	RIA1	1.37	4.89	7.70	0.63	817	622
$\Delta\%$	BM0	−29.58	−7.88	−18.25	−12.60	−2.89	−0.76
	BM0.1	−22.25	−13.10	−17.11	−6.67	−4.99	−1.48
	BM1	−28.16	−4.11	−19.97	−14.81	−6.84	−5.94
	RIA0	−13.18	−4.27	−20.04	−5.93	−4.06	−9.99
	RIA0.1	−30.72	−11.09	−24.77	−10.99	−8.24	−6.79
	RIA1	−15.52	−16.05	−29.41	−1.06	−13.92	−18.94
p	BM0	<0.001*	0.052	<0.001*	0.001*	0.443	0.705
	BM0.1	0.003*	0.004*	<0.001*	0.087	0.077	0.474
	BM1	<0.001*	0.107	<0.001*	<0.001*	0.057	0.002*
	RIA0	0.006*	0.229	<0.001*	0.063	0.280	<0.001*
	RIA0.1	<0.001*	0.029*	<0.001*	0.006*	0.048*	0.002*
	RIA1	0.016*	0.004*	<0.001*	0.755	0.013*	<0.001*

100 μm is necessary to provide enough space for vascularization of the scaffold, one of the key features of scaffolds.[12] Pores of more than 500 μm diameter are too big to provide intercellular contact.[12] SS, a parameter representing the surface of the scaffold, also showed a substantial decrease in RIA0. A decrease in the porous surface is induced by embedding structure within the cavities–bone formation in pores reduces SS.[2] TV, SV, and P decreased more in BM0. TV outlines the whole implant, including soft tissue; SV represents only the scaffold itself. *P* is calculated by the ratio of TV to the volume of empty spaces within the construct; *P* depends on both TV and SV. TV always comes with a certain inaccuracy: bone formation is located around the β-TCP-granules and not within the surrounding soft tissue – this inaccuracy also applies to *P*[2].

BMP-7 stimulation was followed by more bone formation in both groups compared to cell-seeded implants that were not stimulated. This proofs previously published *in vitro* findings.[6] SS and PN decreased more sharply in BM1, RIA0.1, and RIA1 compared to BM0 and RIA0. Overall, hRIA-MSC seemed to react more sensitively to stimulation by BMP-7. The higher the dose of BMP-7, the more SS and PN declined. Furthermore, RIA-constructs the decline in SS is parallel to BMP-7-application. For hBMSC-seeded scaffolds, changes for SS remained on the same level, independent from the stimulating dose.

The amount of rPN in PN decreased for RIA0 and RIA1; only small changes were detectable in BM1 and RIA0.1[7]: bone ingrowth fills the smallest pores completely with bone. This means that they "disappear" in T1 whereas they are counted in T0. Bigger pores would not be filled with new bone completely: a smaller pore remains. These pores are counted as pores in T1 as well, but within a smaller subset of pores compared to T0 (Fig. 2b). It should be assessed whether a longer implantation period promotes further filling of those pores. Furthermore, bone formation leads to stabilization of the constructs' structural integrity. Minimal bone formation cases mechanical compaction of the scaffold and analyzed by a decrease of rPN in T1 compared to T0: especially the pores between the granules are influenced by mechanical destruction. By using β-TCP-granules bonded together with Fibrin-Thrombin-glue, we created a new subset of pores with undefined pore diameter.

By assuming the change of rPN, SS, and SV being the most important correlates of bone-formation in mCT-evaluation, BMP-7 has a positive effect on the amount of newly built bone. The same result was obtained by qualitative mCT-evaluation. Furthermore, RIA-constructs react more sensitively to BMP-7-application. Even low-dose stimulation is followed by increased bone formation.

BMP-2 is applied routinely for the treatment of bone defects as well as in combination with autologous bone.[16] It would be interesting to compare the osteostimulative effects of BMP-2 to those of BMP-7 by using our model. Insulin-like growth factor (IGF)-1 showed promising results in clinical studies and could also be evaluated with our model.[2,17] Furthermore, β-TCP-granules should be replaced by either solid β-TCP-scaffolds to provide a more standardized model or alternative bone substitutes like bioactive glasses, which can be tested within the experimental model described.[7,18] Another promising way to stimulate bone formation clinically could be the use of the patient's own platelet-rich plasma (PRP), containing a physiological mix of a lot of growth and differentiation factors.[19] PRP could be a promising alternative to commercially available recombinant differentiation factors, especially in combination with new bone scaffold substitutes.[20,21] Further clinical studies are necessary to evaluate the effect of PRP on bone regeneration, for example, by using serum cytokine expression course assays.[2]

5. Conclusions

Our results demonstrated that quantitative mCT-analysis is a valid and reliable tool for evaluating bone formation. The use of mCT in observational studies allows for the evaluation of bone formation as well as the reduction animals used. Furthermore, we could show that hMSC isolated from reaming material has a high osteogenic potential *in vivo*, especially in comparison to hBMSC. BMP-7 stimulation of bone formation is more effective for hRIA-MSC, even when using small doses.

Conflicts of interest

The authors have none to declare.

References

1. Moghaddam A, Zietzschmann S, Bruckner T, Schmidmaier G. Treatment of atrophic tibia non-unions according to 'diamond concept': results of one- and two-step treatment. *Injury.* 2015;46(suppl 4):S39–S50.
2. Westhauser F, Zimmermann G, Moghaddam S, et al. Reaming in treatment of non-unions in long bones: cytokine expression course as a tool for evaluation of non-union therapy. *Arch Orthop Trauma Surg.* 2015;135:1107–1116.
3. Giannoudis PV, Einhorn TA, Schmidmaier G, Marsh D. The diamond concept – open questions. *Injury.* 2008;39(suppl 2):S5–S8.
4. Kuehlfluck P, Moghaddam A, Helbig L, Child C, Wildemann B, Schmidmaier G. RIA fractions contain mesenchymal stroma cells with high osteogenic potency. *Injury.* 2015;46:S2–S11.
5. Zimmermann G, Moghaddam A. Allograft bone matrix versus synthetic bone graft substitutes. *Injury.* 2011;42(suppl 2):S16–S21.
6. Zhi L, Chen C, Pang X, Uludag H, Jiang H. Synergistic effect of recombinant human bone morphogenic protein-7 and osteogenic differentiation medium on human bone-marrow-derived mesenchymal stem cells in vitro. *Int Orthop.* 2011;35:1889–1895.
7. Westhauser F, Weis C, Hoellig M, et al. Heidelberg-mCT-Analyzer: a novel method for standardized microcomputed-tomography-guided evaluation of scaffold properties in bone and tissue research. *R Soc Open Sci.* 2015;2:150496.
8. World Medical A. World Medical Association Declaration of Helsinki: ethical principles for medical research involving human subjects. *JAMA.* 2013;310:2191–2194.
9. Moghaddam A, Weiss S, Wolfl CG, et al. Cigarette smoking decreases TGF-b1 serum concentrations after long bone fracture. *Injury.* 2010;41:1020–1025.
10. Dominici M, Le Blanc K, Mueller I, et al. Minimal criteria for defining multipotent mesenchymal stromal cells. The International Society for Cellular Therapy position statement. *Cytotherapy.* 2006;8:315–317.
11. Bouxsein ML, Boyd SK, Christiansen BA, Guldberg RE, Jepsen KJ, Muller R. Guidelines for assessment of bone microstructure in rodents using micro-computed tomography. *J Bone Miner Res.* 2010;25:1468–1486.
12. Karageorgiou V, Kaplan D. Porosity of 3D biomaterial scaffolds and osteogenesis. *Biomaterials.* 2005;26:5474–5491.
13. Mills LA, Simpson AH. In vivo models of bone repair. *J Bone Joint Surg Br.* 2012;94:865–874.
14. Wiltfang J, Merten HA, Schlegel KA, et al. Degradation characteristics of alpha and beta tri-calcium-phosphate (TCP) in minipigs. *J Biomed Mater Res.* 2002;63:115–121.
15. Haynesworth SE, Goshima J, Goldberg VM, Caplan AI. Characterization of cells with osteogenic potential from human marrow. *Bone.* 1992;13:81–88.
16. Schmidmaier G, Moghaddam A. Long bone nonunion. *Z Orthop Unfall.* 2015;153:659–676.
17. Fischer C, Doll J, Tanner M, et al. Quantification of TGF-ss1, PDGF and IGF-1 cytokine expression after fracture treatment vs. non-union therapy via masquelet. *Injury.* 2015.
18. Westhauser F, Weis C, Prokscha M, et al. Three-dimensional polymer coated 45S5-type bioactive glass scaffolds seeded with human mesenchymal stem cells show bone formation in vivo. *J Mater Sci Mater Med.* 2016;27:119.
19. Schmidmaier G, Herrmann S, Green J, et al. Quantitative assessment of growth factors in reaming aspirate, iliac crest, and platelet preparation. *Bone.* 2006;39:1156–1163.
20. Oryan A, Alidadi S, Moshiri A. Platelet-rich plasma for bone healing and regeneration. *Expert Opin Biol Ther.* 2016;16:213–232.
21. Gabbai-Armelin PR, Souza MT, Kido HW, et al. Characterization and biocompatibility of a fibrous glassy scaffold. *J Tissue Eng Regen Med.* 2015.